Tellus SERIES A DYNAMIC METEOROLOGY AND OCEANOGRAPHY
PUBLISHED BY THE INTERNATIONAL METEOROLOGICAL INSTITUTE IN STOCKHOLM

Tellus (2009), 61A, 417–427

TELLUS

Tropical large-scale circulations: asymptotically non-divergent?

By JUN-ICHI YANO[1]*, SANDRINE MULET[2] and MARINE BONAZZOLA[2], [1]*CNRM–GAME (Météo-France, CNRS), 31057 Toulouse, France;* [2]*Laboratoire de Météorologie Dynamique, CNRS/UPMC, 75252 Paris, France*

(Manuscript received 10 March 2008; in final form 27 January 2009)

ABSTRACT

Although the large-scale tropical atmospheric circulations are often considered as primarily divergent, a simple scale analysis, originally presented by Charney (1963), suggests otherwise—a dominance of vorticity over divergence. The present paper quantitatively documents the asymptotic non-divergence of the large-scale tropical atmosphere, in association with Madden–Julian oscillations, with use of the Tropical Ocean Global Atmosphere—Coupled Ocean Atmosphere Response Experiment, Large-Scale Array (TOGA–COARE LSA) data set.

The vorticity is larger than the divergence at the majority (70%–80%) of points at any instant for the levels between 850 and 250 hPa, and the vorticity is more than 10 times stronger than the divergence both at 850 and 500 hPa more than half of the time. The root mean square (rms) ratio between the transient components of divergence and vorticity, which is defined as the deviation from the mean for the whole data period, decreases substantially with increasing horizontal scales from 100 to 2000 km, over an intraseasonal timescale (20–100 d). The analysis suggests that the Madden–Julian oscillations are dominated more by vorticity than divergence and more so than at the smaller scales.

The analysis as a whole suggests the feasibility of constructing an asymptotically non-divergent theory for large-scale tropical circulations. A brief sketch of the formulation is presented.

1. Introduction

A popular view of large-scale tropical circulation could be symbolized by a global satellite image showing extensive moist convective activity over the tropics. This activity is associated with strong latent heating, which in turn induces strongly divergent flow. However, the tropical large-scale circulation is likely not as strongly divergent as it appears, as originally pointed out by Charney (1963).

Charney (1963) showed this point by a simple scale analysis as reproduced here, generalizing it to the diabatic case. Charney considered only the adiabatic case. His conclusion does not change by adding the diabatic heating because the latter effect is relatively weak in the large-scale average considered here.

Let a typical horizontal scale of the large-scale tropical circulations be $L \sim 1000$ km, a vertical scale $H \sim 10$ km, a horizontal velocity $U \sim 10\,\mathrm{m\,s^{-1}}$, a typical vertical gradient of the potential temperature $\mathrm{d}\theta/\mathrm{d}z \sim 3\ \mathrm{K\,km^{-1}}$ and a diabatic heating rate $Q \sim 3\,\mathrm{K\,d^{-1}} \sim 3 \times 10^{-5}\,\mathrm{K\,s^{-1}}$, where $1\ \mathrm{d} \sim 10^5$ s. Here, diabatic heating represents both radiative and latent heating associated with moist convection. More precisely, diabatic heating as defined here must be interpreted as a quantity averaged over a large horizontal scale (the order of magnitude of L), also including the transport by eddies not explicitly represented in the large-scale average, more formally defined as the apparent heat source by Yanai et al. (1973).

The argument hinges strongly on an observationally well-known thermodynamic balance in the large-scale tropical atmosphere between the vertical advection and diabatic heating Q:

$$w(\mathrm{d}\theta/\mathrm{d}z) \simeq Q, \tag{1}$$

where w is the vertical velocity (e.g. Mapes and Houze, 1995; Frank and McBride, 1989; Yano, 2001; see fig. 1 of Yano in particular). Sobel et al. (2001) proposed calling this balance (eq. 1) the weak temperature gradient (WTG) approximation. Under this balance, the order of magnitude W of the vertical velocity is estimated as

$$W \sim Q/(\mathrm{d}\theta/\mathrm{d}z). \tag{2}$$

*Corresponding author.
e-mail: yano@cnrm.meteo.fr
DOI: 10.1111/j.1600-0870.2009.00397.x

Consequently, the magnitude of horizontal divergence is estimated by

$$\nabla \cdot \mathbf{v}_H \sim W/H \sim [Q/(\mathrm{d}\theta/\mathrm{d}z)]/H \sim (3 \times 10^{-5}/3 \times 10^{-3})/10^4 \sim 10^{-6}\,\mathrm{s}^{-1}, \quad (3)$$

whereas a direct estimate of the horizontal divergence from the horizontal velocity is given by

$$\nabla \cdot \mathbf{v}_H \sim U/L \sim 10/10^6 \sim 10^{-5}\,\mathrm{s}^{-1}. \quad (4)$$

Clearly, this direct estimate of divergence is too strong to be balanced by diabatic heating, indicating that the tropical large-scale circulation is, in fact, non-divergent to a leading order. We call this notion 'asymptotic non-divergence', which we examine by data analysis in the present paper.

The order of magnitude of vorticity is estimated in the same manner as for the horizontal divergence by U/L (cf. eq. 4). However, we do not see any physical constraint that further limits the magnitude of vorticity, thus it is reasonable to anticipate that the order of magnitude of the vorticity remains U/L. Hence, a simple corollary of asymptotic non-divergence is that the tropical large-scale circulations are dominated by vorticity more than divergence.

Sardeshmukh and Hoskins (1987) originally made this argument and extensively documented this point for climatological circulations, but they presented only one instantaneous field at the synoptic timescale (their fig. 13). A systematic analysis of asymptotic non-divergence is yet to be performed for the synoptic scale. This is a specific goal of the present paper.

The Tropical Ocean Global Atmosphere—Coupled Ocean Atmosphere Response Experiment (TOGA–COARE) Large-Scale Array (LSA) data set is employed for this purpose (cf. Webster and Lukas, 1992). The data set is described in the next section. A synoptic overview during TOGA–COARE is presented in Section 3, particularly in the context of the Madden–Julian oscillations (MJO). A statistical analysis is presented in Section 4 to further quantify a tendency towards asymptotic nondivergence. Results are discussed in Section 5.

The MJO and other so-called convectively coupled equatorial waves (cf. Wheeler and Kiladis, 1999) provide particular motivation for the present study because the associated vorticity fields are rarely examined. If these variabilities are indeed vorticity dominated, not only must the strategy for data analysis be modified, but there will be a need also for developing a new type of theory.

The present analysis supports the idea that the large-scale tropical atmosphere can be treated as non-divergent to a leading order of asymptotic approximation (cf. Bender and Orszag, 1978). In other words, large-scale tropical circulations are primarily dictated by a vorticity conservation law (see eq. 5 below), in the same manner as the mid-latitude large-scale circulations are dictated by a potential vorticity conservation law (cf. Hoskins et al., 1985). This point of view is qualitatively different from the traditional view based on equatorial waves (cf. Wheeler and Kiladis, 1999).

Of course, asymptotic non-divergence does not mean that divergence plays no role at all. On the contrary, important effects of weak non-divergence associated with moist convection are taken into account as a slow timescale process at a higher order of asymptotic expansion. As a result, the divergent field plays a catalytic role in large-scale tropical circulations.

We believe that a much more lucid theory for large-scale tropical circulations could be developed under the asymptotic non-divergence hypothesis. Though a development of a complete theory is beyond the scope of the paper, a brief sketch of the formulation is presented in Section 6 in concluding the paper. The significance of the vorticity conservation law for the large-scale tropical atmospheric dynamics is also discussed in the last section.

2. Data set

A gridded data set over the LSA domain during the TOGA–COARE Intensive Observing Period (IOP 1 November 1992–28 February 1993) is used for the present study. The data set was processed at the Colorado State University and it is available at http://tornado.atmos.colostate.edu/togadata/gridded.html. In constructing this data set, the merged profiler/rawinsonde data set (Ciesielski et al., 1997) and sounding data from other priority sounding sites have been used. In performing multiquadric interpolation (cf. Nuss and Titley, 1994), the gridded fields are constructed at 25 hPa vertical resolution from 1000 to 25 hPa and at 1° resolution, both in longitude and latitude. The analysis domain spans 140°E–180°E in longitude, 10°S–10°N in latitude.

For the present study, both divergence δ and vorticity ζ are calculated from the horizontal wind components using a standard centered difference scheme. An objectively diagnosed divergence field δ_D that removes potential systematic errors is also provided as part of data product (cf. Haertel, 2002); however, no equivalent correction for vorticity is available. For consistency in the treatment of the two variables, the corrected divergence field is not used in the present study.

A linear regression shows that the two diagnosed divergence fields are best fit by

$$\delta_D = 1.013\delta + 2.190 \times 10^{-8},$$

with the correlation coefficient 0.996 for the whole domain and period of the data.[1] Hence, for the present statistical analyses,

[1] A discrepancy is partially due to different grids used in evaluating the divergence. The diagnosed divergence provided on the web is evaluated using winds objectively interpolated onto the Arakawa's C-grid, on which the winds are staggered at half gridpoints relative to the the other variables. The wind values are later re-interpolated onto the same whole gridpoints as the other variables for public release (Paul Ciesielski, personal communication, December 2007).

the results are insensitive to the choice of divergence data. Furthermore, to avoid possible systematic errors, some analyses are repeated by taking an average of 2×2 gridpoints with basically no change in the results (cf. Section 4.2 below).

The TOGA–COARE data set is chosen because of its easy accessibility, and, more importantly, because of our preference for statistically analyzed data over assimilated data, to avoid the possible biases from the physical parametrizations of the global model on which the assimilation is based. Though it is too naive to imagine that the statistical analysis data are not prone to errors (cf. Mapes et al., 2003), we believe, as discussed above, that the present statistical analysis is not strongly affected by these errors.

3. Synoptic overview

During the TOGA–COARE period, two MJO events are identified (see e.g. fig. 3 of Yanai et al., 2000). The first MJO passed over the Indian Ocean to the Western Pacific Ocean from mid December to early January. The second occurred in February. The evolution of the divergence and the vorticity fields associated with the two MJO events is shown Figs. 1 and 2, respectively, as height-longitude sections. The first two panels (a) and (b) show the two periods prior to the arrival of the MJO events into the LSA region. The last two panelss (c) and (d) show the fields during the first and the second MJO over LSA, respectively. The only strong signal of divergence is seen at the tropopause level. On the other hand, the signal of vorticity extends over the whole troposphere with a maximum at the 850 hPa level. The divergence field is clearly much weaker than the vorticity field over the whole troposphere during the two MJO events. In other words, vorticity dominates divergence during the MJO. On the other hand, the dominance of vorticity over divergence is less clear during pre-MJO periods, when both fields are substantially suppressed.

The time-longitude sections of the two fields are shown Fig. 3, panel (a) the vorticity at 850 hPa and panel (b) the divergence at 150 hPa. The level with the strongest divergence is chosen in this comparison. Recall that the divergent field is much weaker at lower levels. Inspection of Fig. 3 shows that the magnitude of the divergence is always weaker than that of the vorticity, in spite of the fact that the vertical level with the strongest divergence is taken for the comparison. Hence, contrary to the common notion, vorticity dominates divergence in the tropical large-scale circulations associated with the occurrence of MJO.

However, the two fields associated with the MJO events (indicated by OLR in Fig. 3) are clearly correlated and propagate together eastwards. The tendency is particularly clear for the first

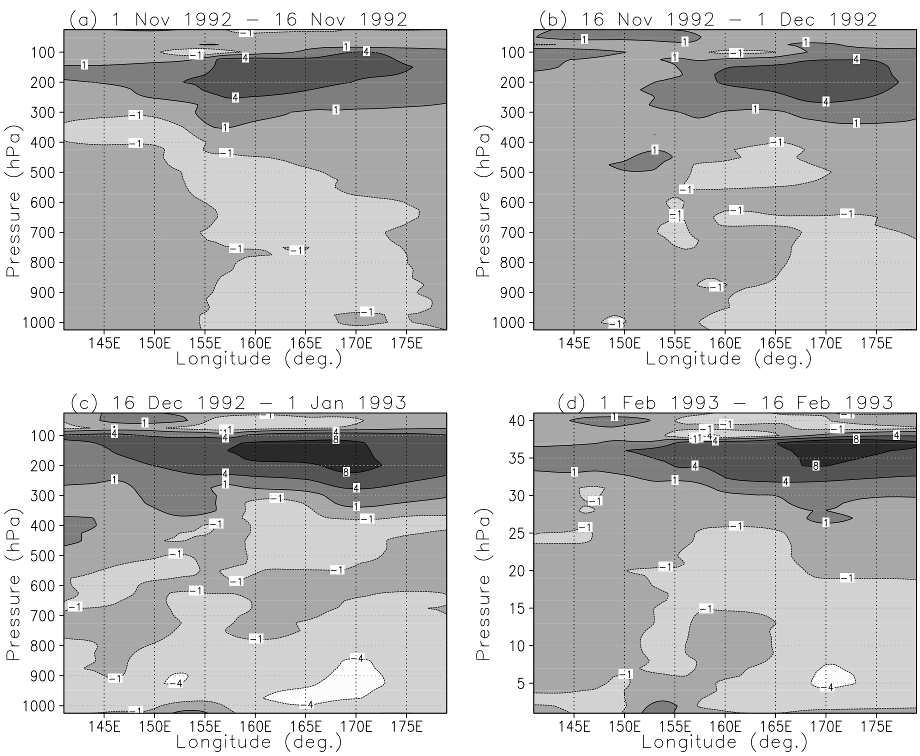

Fig. 1. Height-longitude sections of the divergence field averaged over 5°S–5°N for time average of the periods: (a) 1–16 November 1992; (b) 16 November–1 December 1992; (c) 16 December 1992–1 January 1993 and (d) 1–16 February 1993. The divergence is shown by grey tones with values indicated in unit of 10^{-6} s^{-1}.

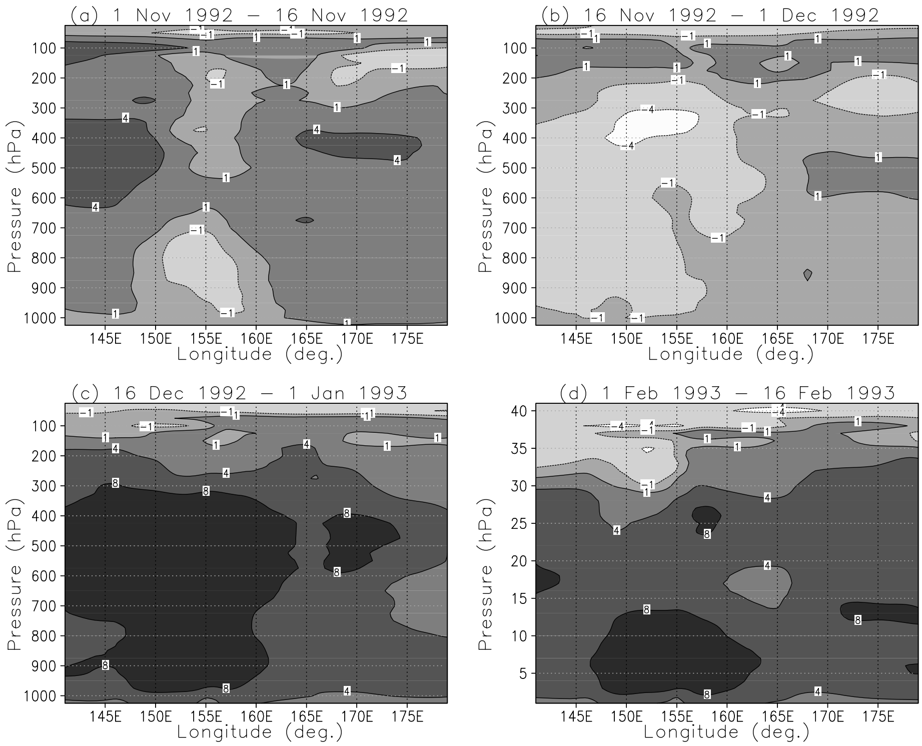

Fig. 2. The same as Fig. 1 but for the vorticity field. Note that the grey tones are given in the same scale as for Fig. 1 so that a direct comparison of the two fields is possible.

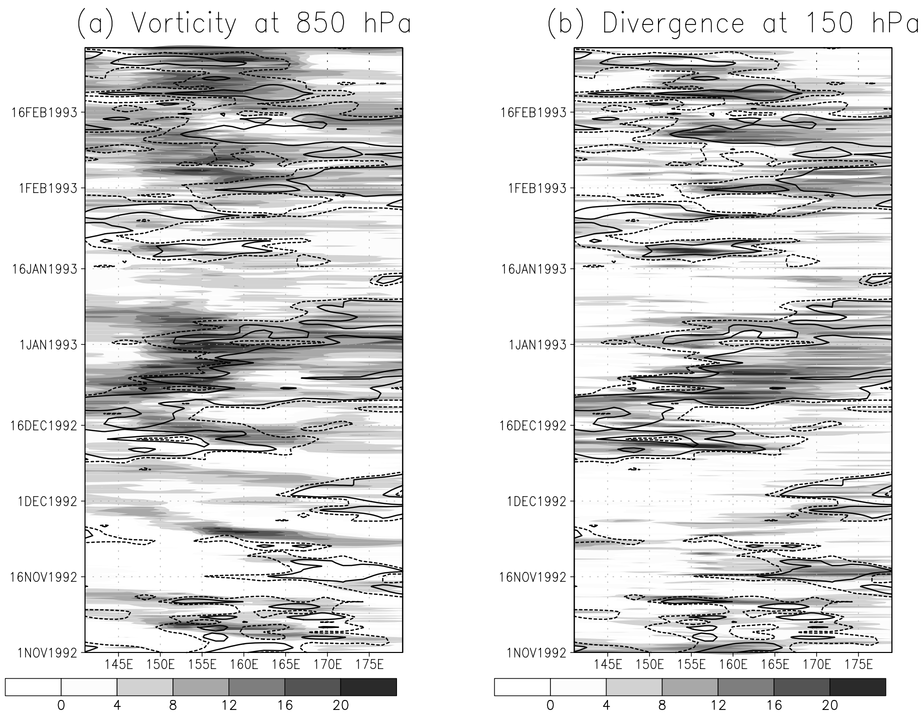

Fig. 3. Time-longitude sections of (a) the vorticity at 850 hPa and (b) the divergence at 150 hPa averaged over 5°S–5°N. Values of the two fields are indicated by grey tones defined by the tone bar at the bottom in unit of 10^{-6} s^{-1}. Note that the same scale range is used for the two fields for easy comparisons of the magnitudes. Superposed on both frames are OLR averaged over 5°S–5°N with solid (180 W m^{-2}) and dashed (200 W m^{-2}) curves.

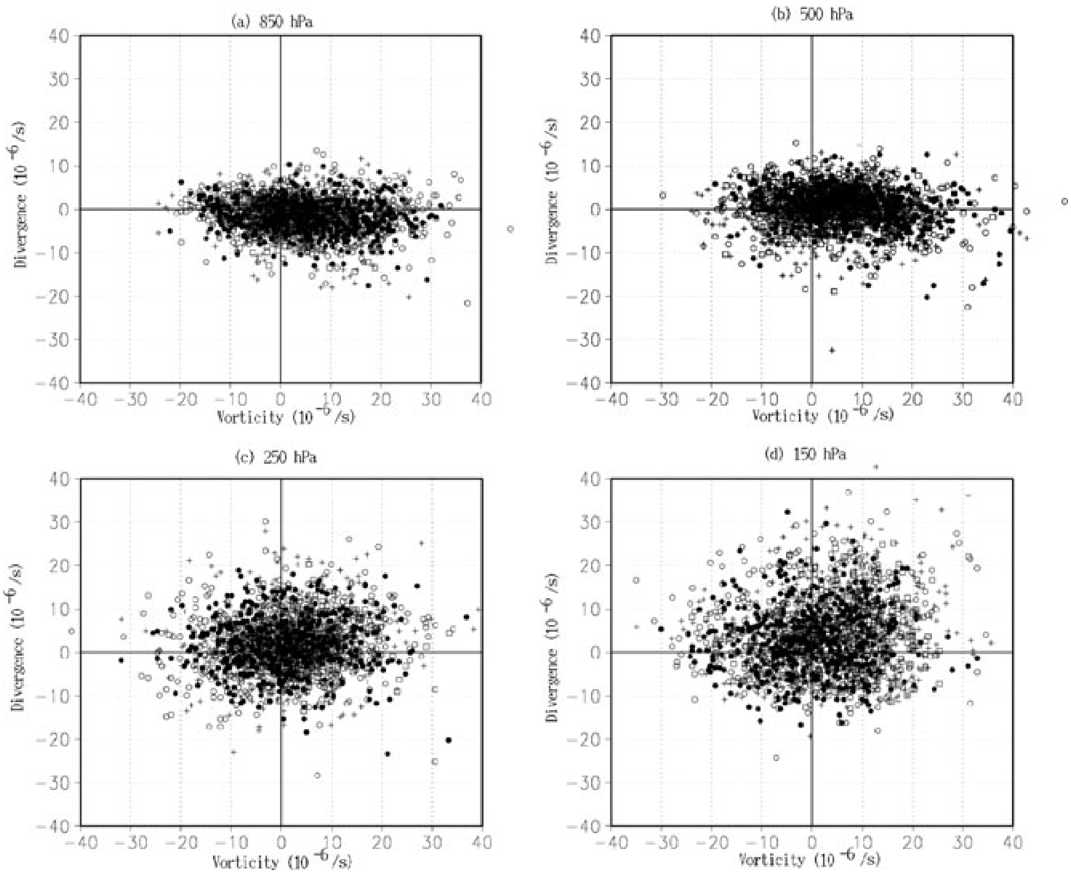

Fig. 4. Scatter plots between the vorticity (horizontal axis) and the divergence (vertical axis) over the IFA region at (a) 850, (b) 500, (c) 250 and (d) 150 hPa. The four gridpoints (151°E, 3°S), (153°E, 3°S), (151°E, 1°S) and (153°E, 1°S) over the IFA region are plotted with varying symbols.

event from mid December to early January, however, less so for the second due to its stalling after reaching the LSA region (cf. fig. 3 of Yanai et al., 2000).

The divergence field tends to be in phase with the convection maximum (corresponding to the OLR minimum), whereas the vorticity field is slightly lagged behind, presumably being induced by the divergence. Thus, though the divergence field is weak, it has a catalytic role in controlling the vorticity field.

We also presume that the vorticity field is associated with the double Rossby vortices in the Gill (1980) solution as indicated by, for example, figs. 7 and 8 of Yanai et al. (2000). Unfortunately, due to a limited latitudinal span (10°S–10°N) of the LSA data adopted here, we cannot examine the whole structure of the Rossby vortices.

4. Statistical analysis

4.1. Scatter plots

To better quantify the tendency towards asymptotic non-divergence suggested in the previous section, some statistical analyses are presented in this section. Probably the most intuitive way to see a relative magnitude of the two variables is to consider scatter plots (e.g. Yano, 2001).

The scatter plots between vorticity and divergence at four gridpoints (151°E, 3°S), (153°E, 3°S), (151°E, 1°S) and (153E, 1S) over the Intensive Flux Array (IFA) region are presented Fig. 4 for the four vertical levels: (a) 850; (b) 500; (c) 250 and (d) 150 hPa. Note that the whole IOP is used for the plots. For the 850–250 hPa levels, the scatter plot is dominated by horizontal spread (the axis for vorticity) rather than vertical spread (the axis for divergence), although this is less obvious at 250 hPa. On the other hand, at 150 hPa, the magnitudes of the two variables become almost comparable.

4.2. Cumulative probability

The tendency toward asymptotic non-divergence is further quantified by the cumulative probability of the absolute ratio of the divergence δ to the vorticity ζ, $|\delta/\zeta|$, as shown Fig. 5. The whole LSA data set is used as a sample space. The vertical axis (cumulative probability) shows the probability that the ratio $|\delta/\zeta|$ is less than the reference ratio given by the horizontal axis for two different ranges in panels (a) and (b). The majority of points

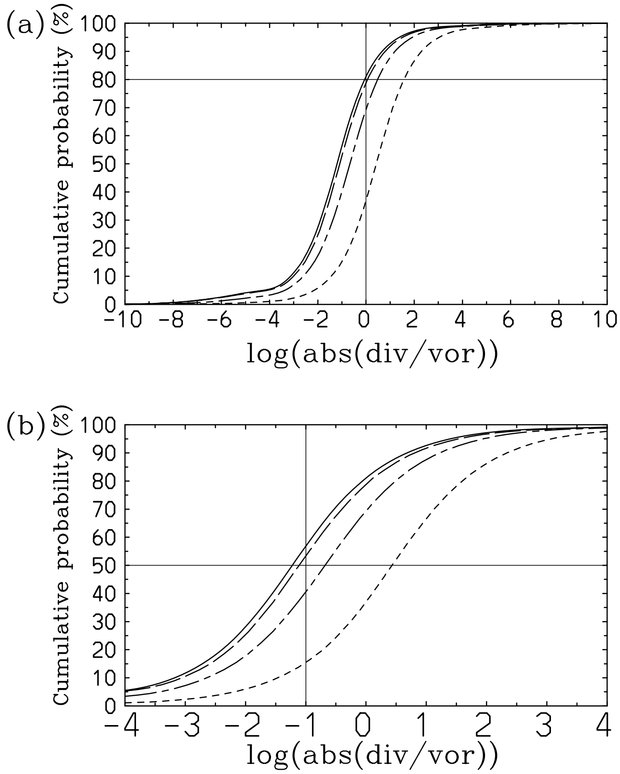

Fig. 5. Cumulative probability distributions for the absolute ratio of the divergence δ to the vorticity ζ, $|\delta/\zeta|$, at 850 (solid curve), 500 (long-dashed), 250 (chain-dashed) and 150 hPa (short-dashed). The sample is for the whole LSA data set. The probability is shown in two different ranges for (a) $\log|\delta/\zeta| = [-10, 10]$ and (b) $[-4, 4]$, respectively, to see a global structure as well as a local structure around $\log|\delta/\zeta| \sim 0$.

are characterized by an absolute value of vorticity larger than divergence between 850 and 250 hPa. These points constitute more than 80% of the total both at 850 (solid curve) and 500 hPa (long-dashed) and more than 70% at 250 hPa (short-dashed).

Even the chance that vorticity is 10 times stronger than divergence (i.e. $\log|\delta/\zeta| = -1$) is quite high, with the probabilities of 59.1%, 55.6% and 42.7%, respectively, at the 850, 500 and 250 hPa levels. The maximum of the probability density, defined as a function of $\log(|\delta/\zeta|)$, is reached at $|\delta/\zeta| = 0.04$, 0.04 and 0.25, respectively, at 850, 500 and 250 hPa.[2] Note that the corresponding values are 0.06, 0.1 and 0.25 when the 2×2 gridpoint average is applied.

[2] When a dependent variable for the probability density p is chosen either as $|\delta/\zeta|$ or $|\zeta/\delta|$, the maximum is found at zero, because the probability density for $\log(|\delta/\zeta|)$ does not decay fast enough towards both directions of the tails. Note that the probability densities $p(|\delta/\zeta|)$, $p(|\zeta/\delta|)$, defined as functions of these ratios are related to the one defined as a function of $\log(|\delta/\zeta|)$ by $p(|\delta/\zeta|) = |\zeta/\delta|\, p(\log(|\delta/\zeta|))$ and $p(|\zeta/\delta|) = |\delta/\zeta|\, p(\log(|\delta/\zeta|))$.

On the other hand, asymptotic divergence at the level of tropopause (150 hPa) is no longer clear—only 40% of the data present stronger vorticity than divergence.

4.3. RMS ratio

Another way of quantifying the dominance of vorticity over divergence is to take the ratio between the root mean square (rms) of divergence and of vorticity, that is, $\langle\delta^2\rangle^{1/2}/\langle\zeta^2\rangle^{1/2}$, where $\langle\ \ \rangle$ designates the space and time mean of a variable over the whole LSA data set for a given vertical level. The rms ratio is found to be 0.36 at 850 hPa, 0.40 at 500 hPa and 0.59 at 250 hPa.

These values are not as small as suggested by the probability analysis, though the two analyses do not quantify the same aspect of asymptotic non-divergence. The rms ratio measures a mean relative spread of the two variables, whereas the probability analysis identifies a likely instantaneous ratio.

Comparison of the two analyses suggests that divergence is more likely to be weaker than average, when vorticity is stronger. This is consistent with the time-longitude section in Fig. 3, which shows that vorticity tends to lag divergence. On the other hand, a relatively large rms ratio suggests that there is still a substantial number of strongly divergent events.

4.4. Time-space scale dependence: total components

Strongly divergent events are likely to be sporadic and associated with short timescale and small spatial-scale convective variabilities. Thus, they would be relatively easily filtered out by applying time and space averages, whereas the magnitude of the vorticity field would diminish less with averaging, being dominated by larger-scale features.

To test this interpretation, a moving average is applied in both time and space simultaneously to divergence and vorticity, then the ratio of the rms is evaluated. Here, the space averaging is performed over square domains with an equal distance, in degrees, in both longitude and latitude. The horizontal distance in latitude is translated into the unit of km in presenting the results.

Figure 6 shows the rms ratio at 850 hPa as a function of both time- and space-scale averaging. The time-averaged rms ratio decreases over the first few days by one third, then the ratio gradually approaches a constant 0.24 with increasing timescales and a fixed spatial scale below 400 km. The tendency at larger horizontal scales is much less intuitive: the rms ratio increases with increasing horizontal scales with the tendency more pronounced at scales longer than few days.

4.5. Time-space scale dependence: transient components

We speculate that the non-vanishing tendency of divergence in the long timescale limit is due to a contribution of the time-mean

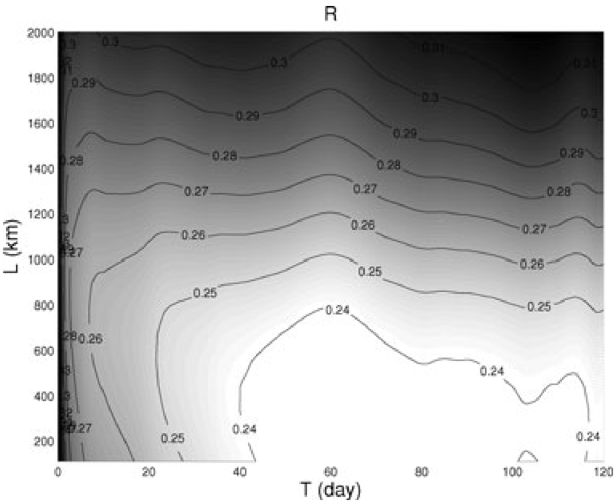

Fig. 6. RMS ratio of the divergence to the vorticity, that is, $\langle\delta^2\rangle^{1/2}/\langle\zeta^2\rangle^{1/2}$ at 850 hPa, as functions of the averaging scales in time (horizontal axis) and horizontal scale (vertical axis).

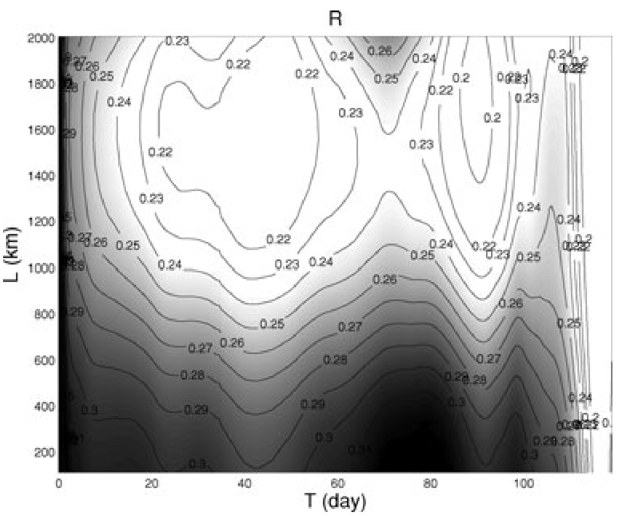

Fig. 7. The same as Fig. 6 but for the transient components $\langle\delta'^2\rangle^{1/2}/\langle\zeta'^2\rangle^{1/2}$, where the prime indicates a deviation from the time mean.

Hadley–Walker circulation, which is inherently divergent. To test this hypothesis, the analysis is repeated for transient components, subtracting the time means, of both divergence and vorticity.

The result presented Fig. 7, however, shows by contradicting the hypothesis that the rms ratio for the transient components decreases much slower with increasing timescales than that for the total component for the horizontal scales less than 800 km. The ratio remains close to 0.3 up to the 100-day scale, when no spatial average is applied. A sudden decrease above this timescale is remarkable, but it has no statistical significance due to a drastic decrease in sampling size with increased averaging.

A starker contrast to the case with the total component is that the rms ratio decreases with increasing horizontal scales for a range of timescales 20–100 d. The result suggests that the intraseasonal variability associated with the MJO is dominated by vorticity more than synoptic and mesoscale variabilities.

Two well-defined minima at the horizontal scale $\sim$1600 km and at the periods 40 and 90 d are remarkable. Nevertheless, the barrier separating these two peaks is relatively weak (the increase is only 0.02). A statistically independent point representing this barrier is no more than one with no more than two cycles repeated for the given timescale (80 d) over the whole data period. Hence, neither the amplitude nor the degree of freedom representing this barrier is large enough to make it statistically significant.

On the other hand, the broad minimum over the timescales 20–100 d at the horizontal scale $\sim$1600 km is clearly statistically significant. The order of magnitude of the minimum is comparable to the total variance of the rms ratio. Furthermore, we estimate the number of statistically-significant points over the broad minimum, by counting the number of discrete periods available in the Fourier space over the given period range. The degree of freedom approximately equal to 10 provides a sufficiently large "normalized" difference to pass the Student test of significance.

5. Discussion

According to a scale analysis originally presented by Charney (1963), the divergence field on the tropical large-scale (of the order 10^3 km) is about 10 fold smaller than the vorticity field. Hence, the large-scale tropical atmosphere may be treated as non-divergent to a leading order of asymptotic expansion (cf. Bender and Orszag, 1978).

The analysis of the present paper using the TOGA-COARE LSA data set generally supports *asymptotic non-divergence*, showing that divergence is small compared with vorticity. The scatter plots most intuitively demonstrate this point. More quantitatively, at the majority (70%–80%) of points at any instant at the levels between 850 and 250 hPa, vorticity dominates divergence, and more than half of the time, vorticity is more than 10 times stronger than divergence both at the 850 and 500 hPa levels.

On the other hand, the overall ratio of the two fields measured by the rms is just less than a half at 850–250 hPa. Though the obtained ratio is not as small as indicated by the probability analysis, it would still justify the use of an asymptotic expansion with a non-divergent flow to a leading order. A parameter that is small only by a fractional factor is often sufficient for performing an asymptotic expansion (cf. Bender and Orszag, 1978; see also e.g. Yano, 1992 for a specific example), in stark contrast to the notion of an analytical limit. The relatively large ratio compared with the original estimate by Charney (1963) is probably attributed to a large wind-speed scale, $U \sim 10$ m s^{-1}, adopted in his scale analysis.

The change of the degree of asymptotic non-divergence with increasing scales, both in time and space, is investigated by taking the ratio of the rms between divergence and vorticity. Both the total and the transient components are considered. The rms ratio between the total components is expected not to vanish in the limit of long timescale due to the presence of the time-mean Hadley–Walker circulation. This turns out to be the case with a constant 0.24 at 850 hPa. However, even when the time-mean contribution is removed from both divergence and vorticity and only the transient components are considered, the rms ratio does not vanish to a limit of long timescale but approaches a larger constant ($\sim$0.3). The result suggests that the transient component of divergence is more dominant than the total field at all the timescales considered.

Even less intuitive results are found in the tendencies of the change of the rms ratio with increasing horizontal scales: these tendencies are opposite when the total and the transient components are considered. These opposing tendencies may be understood by assuming a balance between vertical advection and diabatic heating in the thermodynamic eq. (1). Then the order of magnitude W of the vertical velocity is estimated by eq. (2) and the divergence by W/H (cf. eq. 3). The order of magnitude of the vorticity is U/L, thus their ratio is estimated by

$$O(\delta/\zeta) \sim (W/H)/(U/L) \sim QL,$$

assuming that $\mathrm{d}\theta/\mathrm{d}z$, H and U do not change with the horizontal scale L.

When the total components are considered, the ratio increases with increasing horizontal scales for all the timescales considered, probably because more or less the same order of magnitude of diabatic heating Q is found for all the horizontal scales considered. It then follows that $O(\delta/\zeta) \sim L$, being qualitatively consistent with the analysis result.

On the other hand, when only the transient components are considered, it appears that the magnitude of Q decreases with increasing horizontal scale L and at a rate faster than the magnitude of vorticity decreases with L. It then follows that the rms ratio for the transient components decreases with increasing horizontal scales, as observed. The result furthermore implies that the so-called convectively coupled equatorial waves such as MJO are dominated by vorticity more than synoptic and mesoscale processes, being consistent with the qualitative analysis presented in Section 3.

A main feature still to be explained in the above interpretation is the tendency of the total diabatic heating rate Q to stay constant with increasing timescales. The simplest explanation would be to assume that the diabatic heating rate follows a $1/f$-noise time-series. The $1/f$-noise refers to a time-series that represents a power spectrum of shape $1/f$, where f stands for frequency (Yano et al., 2001a, 2004). The $1/f$-noise time-series is unique in that its total variability does not change with time averaging (cf. fig. 1 of Yano et al., 2004).

6. Towards an asymptotically non-divergent theory

The question remains: what is the significance of asymptotic nondivergence? How can we describe the large-scale tropical atmosphere consistently under asymptotic non-divergence? In this section, we succinctly address these two issues in subsequent two subsections but with a full description of an asymptotic formulation left for future work.

6.1. Dynamical implications

Asymptotic non-divergence has a very simple dynamic implication: to a first approximation, large-scale tropical circulations may be considered as purely horizontal two-dimensional flows. As for all two-dimensional flows, the vorticity conservation law dictates the evolution of the whole system. In fully non-linear regimes, it further implies that the tropical large-scale circulations can, to a good extent, be understood in terms of two-dimensional turbulence. On an equatorial β-plane, interplays of the inverse cascade and Rossby waves lead to coherent vortices and zonal jets, as for the mid-latitude counterpart (cf. Rhines, 1975). Convection does not play any role in these processes, although it may play a role in generating an initial noise field.

Clearly, asymptotic non-divergence is at odds with the conventional view of the tropical atmosphere, where divergent flows with deep convection dominate. Thus, the next question is: to what extent these effects are negligible and, more importantly, in what way these effects can be incorporated into a framework of asymptotically non-divergent theory? Here, asymptotic non-divergence implies that the circulations may be considered to be non-divergent to leading order, but the catalytic effect of weak divergence can be taken into account as a higher-order effect in the asymptotic expansion.

How can the catalytic role for convectively driven divergent flows be introduced? The original proposal by Charney (1963) was to treat localized strongly divergent convective regions separately under a separate dynamical regimes. Though he stopped short of developing a rigorous formulation, these localized convective regions could be treated, for example, as point-wise, convectively induced vorticity sources of divergence (i.e. the small-scale counterpart of the second term in the left-hand side of eq. 11 below). Here, alternatively, convective forcing of vorticity is treated as a slow timescale process by smoothing these localized divergent fields onto larger scales under a framework of multiscale asymptotic expansion theories, as detailed in the next subsection. We refer to chapter 11 of Bender and Orszag (1978) and section 3.20 of Pedlosky (1987) for the basic notions of the multiscale approaches. Such an asymptotic expansion approach has already been extensively applied to tropical atmospheric large-scale dynamics (e.g. Majda and Klein, 2003; Biello and Majda, 2005).

6.2. Sketch of an asymptotically non-divergent formulation

We consider a primitive equation system in pressure coordinates with the full set of equations as found in any standard textbook (e.g. Holton, 2004). The formulation sketched out in this subsection may be considered as a generalization of the WTG approximation (Sobel et al., 2001) by adding asymptotic non-divergence on top of that.

As originally pointed out by Charney (1963), the system reduces to a non-divergent vorticity equation to leading order with the assumption of asymptotic non-divergence, that is,

$$\left(\frac{\partial}{\partial t} + \mathbf{v}_0 \cdot \nabla\right)(\zeta_0 + f) = 0, \tag{5}$$

where $\mathbf{v}$ is the horizontal wind, f the Coriolis parameter and ∇ refers to a gradient operator on a constant p-surface. All the dependent variables are expanded by a formal expansion parameter, ϵ, which is set equal to one in obtaining the final results (cf. section 31, Schiff, 1968), for example,

$$\zeta = \zeta_0 + \epsilon\zeta_1 + \cdots,$$

with $\nabla \cdot \mathbf{v}_0 = 0$ and $\omega_0 = 0$ by assumption of leading-order non-divergence. Here, ω is the vertical velocity in pressure coordinates. Note that eq. (5) constitutes a closed equation set, that is, under asymptotic non-divergence, the evolution of the large-scale tropical flows is described solely in terms of the vorticity to the leading order, as already emphasized in Section 6.1. Also note that the system described by eq. (5) conserves both kinetic energy and enstrophy, the two important quantities that constraint the cascade tendency of two-dimensional turbulence.

Due to leading-order non-divergence, the divergence equation turns into a diagnostic equation for the geopotential ϕ_0:

$$\nabla^2\phi_0 = -\nabla^2\frac{\mathbf{v}_0^2}{2} + \mathbf{k}\cdot\nabla\times(\zeta_0 + f)\mathbf{v}_0, \tag{6}$$

then the hydrostatic balance

$$\frac{\partial\phi_0}{\partial p} = -\left(\frac{R}{p}\right)\left(\frac{p}{p_0}\right)^{\kappa}\theta_0, \tag{7}$$

in turn, provides the potential temperature θ_0 to the leading order. Here, R is the ideal gas constant, $\kappa = R/C_p$, with C_p the specific heat with the constant pressure, and p_0 a reference pressure. The moisture mixing ratio q_0 may be evaluated by a direct time integration of the full moisture conservation equation

$$\left(\frac{\partial}{\partial t} + \mathbf{v}_0\cdot\nabla + \omega_1\frac{\partial}{\partial p}\right)q_0 = C_0, \tag{8}$$

with a given apparent moisture source C_0. To integrate eq. (8), ω_1 is diagnosed from the thermodynamic balance (WTG approximation):

$$\omega_1(\mathrm{d}\bar{\theta}/\mathrm{d}p) = Q_0, \tag{9}$$

with a basic reference state $\bar{\theta}$ for the potential temperature.

The diabatic heating rate (apparent heat source) Q_0 can be diagnosed from θ_0 and Q_0, in turn, if an appropriate type of convective parameterization such as the Betts–Miller scheme (Betts, 1986) is adopted.

Once ω_1 is diagnosed, then a weak divergence $\nabla\cdot\mathbf{v}_1$ induced by convective heating is diagnosed from mass continuity

$$\nabla\cdot\mathbf{v}_1 = -\frac{\partial\omega_1}{\partial p}. \tag{10}$$

The divergent component $\mathbf{v}_{1,\delta}$ of the first-order flow is obtained by solving eq. (10).

To the first order of the vorticity equation, we include a weak divergence

$$\begin{aligned}&\frac{\partial}{\partial\tau}\zeta_0 + \nabla\cdot[\mathbf{v}_{1,\delta}(\zeta_0 + f)]\\ &\quad = -\left(\frac{\partial}{\partial t} + \mathbf{v}_0\cdot\nabla\right)\zeta_1 - (\mathbf{v}_{1,\zeta}\cdot\nabla)(\zeta_0 + f),\end{aligned} \tag{11}$$

with a slow timescale τ introduced by

$$\frac{\partial}{\partial\tau} = \epsilon\frac{\partial}{\partial t}. \tag{12}$$

Here, ζ_1 is an undetermined first-order vorticity, and $\mathbf{v}_{1,\zeta}$ the first-order rotational wind defined by the former.

Note that the second term on the left-hand side of eq. (11) represents a feedback of weak divergence on the vorticity. Recall that weak divergence is diagnosed from the diabatic heating (convective heating) by eqs. (9) and (10).

According to eq. (11), a weak divergence influences the evolution of the system in two different ways. First, it modifies the leading-order vorticity field ζ_0 slowly with time (the first term). Second, it also induces a weak fast-varying perturbation ζ_1 in the vorticity field (right-hand side).

The main idea of the theory of asymptotic expansions is to derive a closed equation for a slow-evolution of the leading-order vorticity ζ_0, without explicitly solving the evolution of the higher-order fields given in the right-hand side of eq. (11). Such a consistency condition is called 'solvability', which is obtained by multiplying eq. (11) by $\zeta^\dagger$ and integrating it over space (x, y) and time t. Here, $\zeta^\dagger$ is a vorticity solution for the adjoint problem to eq. (5):

$$\begin{aligned}&\triangle\left(\frac{\partial}{\partial t}\zeta^\dagger + \nabla\cdot\mathbf{v}_0\zeta^\dagger\right) + \frac{\partial}{\partial x}\left[\zeta^\dagger\frac{\partial}{\partial y}(\zeta_0 + f)\right]\\ &\quad -\frac{\partial}{\partial y}\left[\zeta^\dagger\frac{\partial}{\partial x}(\zeta_0 + f)\right] = 0.\end{aligned} \tag{13}$$

The initial condition may be set $\zeta^\dagger = \zeta_0$.

The solvability condition for eq. (11) is, as a result, given by

$$\left\langle\zeta^\dagger\frac{\partial}{\partial\tau}\zeta_0\right\rangle + \langle\zeta\dagger\nabla\cdot[\mathbf{v}_{1,\delta}(\zeta_0 + f)]\rangle = 0, \tag{14}$$

assuming either vanishing or periodic boundary conditions for ζ_1. Here, $\langle\quad\rangle$ designates the integral in space (x, y) and time t, changing the definition from Section 4. The integration range may be taken as a whole domain and the maximum period associated with the leading-order solution.

We take a simple separable solution for the leading-order vorticity consisting of the amplitude $Z(\tau)$ for the slow modulation and the fast-evolving part $\tilde{\zeta}_0(x, y, z, t)$:

$$\zeta_0 = Z(\tau)\tilde{\zeta}_0. \tag{15}$$

For the present demonstrative purpose, we assume also a similar separable solution for $\mathbf{v}_{1,\delta}$ (without justification):

$$\mathbf{v}_{1,\delta} = Z(\tau)\tilde{\mathbf{v}}_{1,\delta}. \tag{16}$$

A closed expression for $\mathbf{v}_{1,\delta}$ in terms of leading-order variables may be obtained, once an expression for Q_0 (i.e. convective parameterization) is specified. Some pedagogic examples could be developed by adopting a simple relaxation scheme for Q_0; these examples are left for future work.

Substitution of eqs. (15) and (16) into eq. (14) leads to

$$\frac{dZ}{d\tau} = \alpha Z - \gamma Z^2, \tag{17}$$

with the coefficients defined by

$$\alpha = -\left\langle \zeta^\dagger \nabla \cdot (\tilde{\mathbf{v}}_{1,\delta} f)\right\rangle / \left\langle \zeta^\dagger \tilde{\zeta}_0 \right\rangle, \tag{18}$$

$$\gamma = \langle \zeta^\dagger \nabla \cdot (\tilde{\mathbf{v}}_{1,\delta}\tilde{\zeta}_0)\rangle / \langle \zeta^\dagger \tilde{\zeta}_0 \rangle. \tag{19}$$

To interpret the basic evolution of the system in eq. (17), let us assume that the coefficients α and γ are constant with τ: the vorticity is first amplified where the convergence $-\nabla \cdot \mathbf{v}_1$ is positively correlated with the background planetary vorticity f, providing a positive α. As the vorticity amplifies, it begins to feel a non-linear term proportional to γ, and the disturbance finally approaches an equilibrated amplitude $Z = \alpha/\gamma$, provided $\gamma > 0$. In reality, α and γ depend on τ through $\zeta^\dagger$ by eq. (13); thus, the evolution of the system is more complex.

Through the very crude sketch presented here, we see that under asymptotic non-divergence, the system is completely dictated by a dry fully non-linear non-divergent vorticity eq. (5) to the leading order, then the 'weak' effects of convection are integrated into the system by a slow timescale non-linear amplitude eq. (17). Treatment of dry non-linear dynamics and interactions between convection and the dynamics at two different levels is a clear advantage of the asymptotically non-divergent approach. A formulation sketched here is in stark contrast with the currently dominant view in terms of the convectively coupled equatorial waves (cf. Wheeler and Kiladis, 1999). Many new insights could be yielded by further pursuing this line of investigation.

7. Acknowledgments

The authors acknowledge extensive communications with Pat Haertel concerning the TOGA–COARE LSA data set. Thanks are also due to Laura Davies and Daniel Nethery for their careful reading of the manuscript. S.M. performed most of the work during her 3-month Masters Project. The authors would like to thank Roger Smith and an anonymous reviewer for constructive comments.

References

Betts, A. K. 1986. A new convective adjustment scheme, part I: observational and theoretical basis. *Quart. J. Roy. Meteorol. Soc.* **112**, 677–691.

Bender, C. M. and Orszag, S. A. 1978. *Advanced Mathematical Methods for Scientists and Engineers*, McGraw-Hill, New York, 593 pp.

Biello, J. B. and Majda, A. J. 2005. A new multiscale model for the Madden-Julian oscillation. *J. Atmos. Sci.* **62**, 1694–1721.

Charney, J. G. 1963. A note on large-scale motions in the tropics. *J. Atmos. Sci.* **20**, 607–609.

Ciesielski, P. E., Hartten, L. M. and Johnson, R. H. 1997. Impacts of merging profiler and rawinsonde winds on Toga COARE analyses. *J. of Atmos. Ocean. Tech.* **14**, 1264–1279.

Frank, W. M. and McBride, J. L. 1989. The vertical distribution of heating in AMEX and GATE cloud clusters. *J. Atmos. Sci.* **46**, 3464–3478.

Gill, A. E. 1980. Some simple solutions for heat-induced tropical circulation. *Quart. J. Roy. Meteorol. Soc.* **106**, 447–462.

Haertel, P. 2002. Spurious divergence within objective analyses with application to TOGA COARE heat and moisture budget. In: *Proceedgins of the 25th Conference on Hurricanes and Tropical Meteorology*, 29 April–3 May 2002, San Diego, CA.

Holton, J. R. 2004. *An Introduction to Dynamic Meteorology* 4th Edition, (*International Geophysical Series* Volume 88) Academic Press, San Diego.

Hoskins, B. J., McIntyre, M. E. and Robertson, A. W. 1985. On the use and significance of isentropic potential vorticity maps. *Quart. J. Roy. Meteorol. Soc.* **111**, 877–946.

Majda, A. J. and Klein, R. 2003. Systematic multiscale models for the tropics. *J. Atmos. Sci.* **60**, 393–408.

Mapes, B. E. and Houze, R. A. 1995. Diabatic divergence profiles in Western Pacific mesoscale convection systems. *J. Atmos. Sci.* **52**, 1807–1828.

Mapes, B. E., Ciesielski, P. E. and Johanson, R. H. 2003. Sampling errors in rawinsonde-array budgets. *J. Atmos. Sci.* **60**, 2697–2714.

Nuss, W. A. and Titley, D. W. 1994. Use of multiquadric interpolation for meteorological objective analysis. *Mon. Wea. Rev.* **22**, 1611–1631.

Pedlosky, J. 1987. *Geophysical Fluid Dynamics* 2nd Editoin, Springer-Verlag, New York, 710 pp.

Rhines, P. B. 1975. Waves and turbulence on a β-plane. *J. Fluid Mech.* **69**, 417–443.

Sardeshmukh, P. D. and Hoskins, B. J. 1987. On the derivation of the divergence flow from therotational flow: the χ problem. *Quart. J. Roy. Meteorol. Soc.* **113**, 339–360.

Schiff, L. I. 1968. *Quantum Mechanics* 2nd Edition. McGraw-Hill, New York, 544 pp.

Sobel, A. H., Nilsson, J. and Polvani, L. M. 2001. The weak temperature gradient approximation and balanced tropical moisture waves. *J. Atmos. Sci.* **58**, 3650–3665.

Webster, P. and Lukas, R. 1992. TOGA COARE: the coupled ocean–atmosphere response experiment. *Bull. Am. Meteorol. Soc.* **73**, 1377–1416.

Wheeler, M. and Kiladis, G. N. 1999. Convectively coupled equatorial waves: Analysis of clouds and temperature in the wavenumber–frequency domain. *J. Atmos. Sci.* **56**, 374–399.

Yanai, M. S., Esbensen, S. and Chu, J. H. 1973. Determination of bulk properties of tropical cloud clusters from large-scale heat and moisture budgets. *J. Atmos. Sci.* **30**, 611–627.

Yanai, M., Chen, B. and Tung, W.-W. 2000. The Madden–Julian oscillation observed during the TOGA COARE IOP: global view. *J. Atmos. Sci.* **57**, 2374–2396.

Yano, J.-I. 1992. Asymptotic theory of thermal convection in the rapidly rotating systems. *J. Fluid Mech.* **243**, 103–131.

Yano, J. I. 2001. Residual cumulus parameterization. *Quart. J. Roy. Meteorol. Soc.* **127**, 1261–1276.

Yano, J.-I., Fraedrich, K. and Blender, R. 2001. Tropical convective variability as $1/f$-noise. *J. Clim.* **14**, 3608–3616.

Yano, J.-I., Blender, R., Zhang, C. and Fraedrich, K. 2004. $1/f$ noise and pulse-like events in the tropical atmospheric surface variabilities. *Quart. J. Roy. Meteorol. Soc.* **300**, 1697–1721.